

Formation, Stability, and Mobility of One-Dimensional Lipid Bilayers on Polysilicon Nanowires

Shih-Chieh J. Huang,^{†,‡} Alexander B. Artyukhin,[†] Julio A. Martinez,^{†,§}
Donald J. Sirbulu,[†] Yinmin Wang,[†] Jiann-Wen Ju,[‡] Pieter Stroeve,[§] and
Aleksandr Noy^{*,†}

Chemistry, Materials, and Life Sciences Directorate, Lawrence Livermore National Laboratory, Livermore, California 94550, Department of Civil and Environmental Engineering, University of California Los Angeles, Los Angeles, California 90095, and Department of Chemical Engineering and Materials Science, University of California Davis, Davis, California 95616

Received July 7, 2007; Revised Manuscript Received September 12, 2007

ABSTRACT

Curved lipid membranes are ubiquitous in living systems and play an important role in many biological processes. To understand how curvature and lipid composition affect membrane formation and fluidity, we have assembled and studied mixed 1,2-dioleoyl-*sn*-glycero-3-phosphocholine (DOPC) and 1,2-dioleoyl-*sn*-glycero-3-phosphoethanolamine (DOPE) supported lipid bilayers on amorphous silicon nanowires grown around carbon nanotube cores with controlled wire diameters ranging from 20 to 200 nm. We found that lipid vesicles fused onto nanowire substrates and formed continuous bilayers for all DOPC–DOPE mixtures tested (with the DOPE content of up to 30%). Our measurements demonstrate that nanowire-supported bilayers are mobile, exhibit fast recovery after photobleaching, and have a low concentration of defects. Lipid diffusion coefficients in these high-curvature tubular membranes are comparable to the values reported for flat supported bilayers and increase slightly with decreasing nanowire diameter. A free space diffusion model adequately describes the effect of bilayer curvature on the lipid mobility for nanowire substrates with diameters greater than 50 nm, but shows significant deviations from the experimental values for smaller diameter nanowires.

Lipid membranes of nonplanar shapes are abundant in nature. Numerous reports document their existence in cellular organelles and transient formation in various biological processes.^{1–6} Nonetheless, researchers became interested in the role of the membrane curvature in biology only recently^{7–9} and quickly realized that they need to understand how curvature affects the physical properties of the membrane.^{9–11} Furthermore, curvature can have a profound effect on the bilayer structure: recent experiments demonstrated curvature-directed segregation of lipid mixtures in nonplanar membranes.^{12,13} Fluidity is another critical parameter of biological membranes because mobility of lipids and membrane proteins represents one of the key factors in regulating ligand–receptor interactions, cooperative binding, and aggregation.^{14,15} Earlier experiments on silica bead-supported lipid bilayers^{16,17} indicated that substrate curvature does not significantly influence diffusion of lipid molecules for substrate diameters larger than 0.5 μm . However, we

intuitively expect that differences in packing densities between highly curved and planar membranes would affect membrane fluidity when the radii of the biological membranes drop to a range between 10 and 100 nm. In this size regime, biological membranes frequently form tubular shapes,^{1,3,18–20} yet there are no systematic literature data on lipid mobility for membranes with the curvature in this range.

We report formation and mobility of mixed zwitterionic (DOPC and DOPE) lipid bilayers of different compositions supported on cylindrical hydrophilic nanowire substrates with precisely controlled diameters ranging from 20 to 200 nm. We aim at determining how the shape of lipid molecules along with the substrate curvature affect bilayer stability, its ability to fuse on nonplanar substrates, and the lipid molecule mobility in the resulting supported bilayer membranes. We use fluorescence recovery after photobleaching (FRAP) measurements to show that, for DOPC–DOPE mixtures with DOPE fraction up to 30%, lipid mobility shows a weak increase as the radius of curvature is decreased.

Substrate Design and Fabrication. To characterize membrane properties as a function of curvature, we need to prepare bilayers with measurable, reproducible, and well-

* Corresponding author. E-mail: noy1@llnl.gov.

[†] Lawrence Livermore National Laboratory.

[‡] University of California Los Angeles.

[§] University of California Davis.

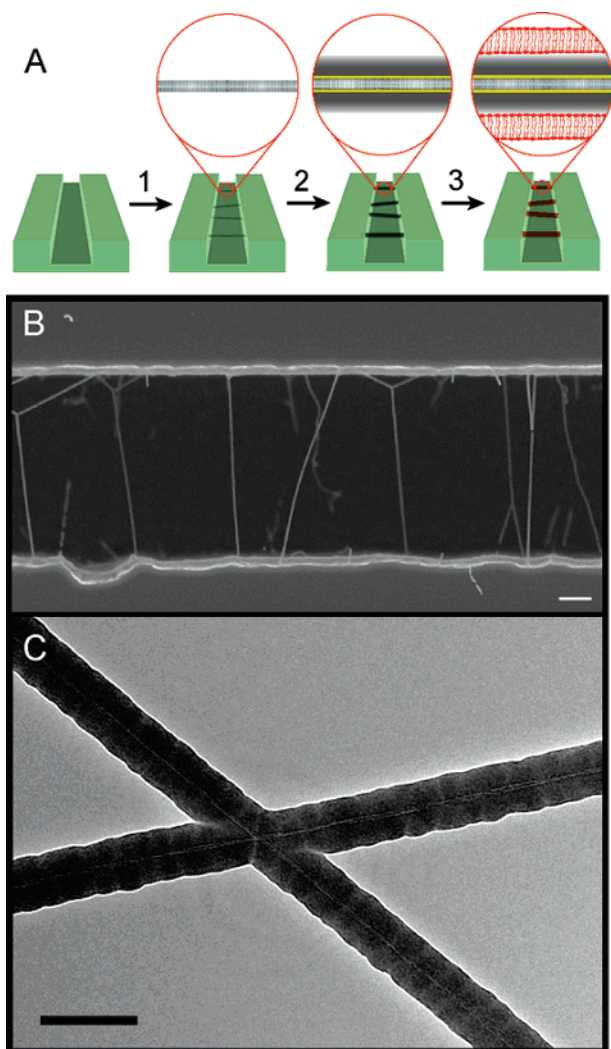


Figure 1. Silicon-coated carbon nanotubes as substrates for studying 1-D lipid bilayers. (A) Schematics of the assembly of lipid bilayer membranes on silicon nanowires. Step 1: CVD growth of suspended carbon nanotubes; step 2: deposition of Ti adhesion layer and amorphous silicon on carbon nanotubes; step 3: formation of supported bilayer by vesicle fusion. (B) SEM image of silicon-coated carbon nanotubes suspended over a 5 μm wide channel. (C) TEM image of two intersecting carbon nanotubes coated with a layer of amorphous silicon. Scale bars: 1 μm (B), 100 nm (C).

controlled curvature. Nonplanar free-standing bilayers, i.e., lipid vesicles, typically do not meet these criteria. Although lipid vesicles are easy to prepare, existing methods give wide, nonuniform distribution of vesicle sizes (and thus curvatures). Our approach utilizes assembly of lipid bilayers on solid substrates of variable curvature. Supported bilayer membranes retain many similarities to natural membranes and, most importantly, their fluidity in the lateral direction.²¹ We chose to use cylindrical amorphous silicon nanowires (with native silicon oxide surface) grown over small diameter carbon nanotubes as the substrates. To ensure complete coating of the lipid around and along the substrates, the nanowires were suspended over a microfabricated trench on a silicon wafer (Figure 1). The outer diameter of these core-shell nanostructures, therefore, defined the membrane curvature and provided a well-characterized chemical surface

(i.e., silicon oxide) that promotes the formation of fluid-supported bilayers.²²

To fabricate amorphous silicon nanowires, we start with CVD growth of single-walled carbon nanotubes suspended across microfabricated channels in Si/SiO₂ (Figure 1a, step 1; see Supporting Information for details). The suspended nanotubes then serve as templates for depositing a layer of amorphous silicon (Figure 1a, step 2), which produces 5 μm long cylindrical silicon wires of 20–200 nm in diameter (Figure 1b,c). The fabrication process is very reproducible: it generates nanowires with ultranarrow diameter distributions and smooth walls (the average width of the diameter distributions was $1.7 \pm 0.9\%$, the maximum measured peak-to-valley surface roughness of the nanowire surface was less than 2 nm, and rms surface roughness for a single nanowire was as small as 0.4 nm). The uniformity of the nanowire substrates produced by our synthesis procedure provides a key advantage for studying curvature effects in supported lipid bilayers. In comparison, catalytic CVD synthesis produces single-crystalline silicon nanowires²³ with atomically smooth surfaces; however the nanowire diameter distribution in CVD samples is usually broad (10–20%) and is mainly determined by dispersion of size of catalyst nanoparticles used for synthesis.²⁴ This distribution would complicate the correlation of membrane properties with the substrate curvature.

Vesicle Fusion on Curved Substrates. To explore the relationship between the shape of lipid molecules and the membrane curvature,^{25,26} we have studied fusion of mixed DOPE–DOPC vesicles on nanowires of various diameters using confocal fluorescence microscopy (Figures 2, 3a). We tested fusion of lipid vesicles with DOPE fraction of 0, 18, 20, 22, and 30 mol %. To visualize formation of supported lipid bilayers, we added 2% of a fluorescent probe 1-oleoyl-2-[6-[(7-nitro-2-1,3-benzoxadiazol-4-yl)amino]hexanoyl]-*sn*-glycero-3-phosphoethanolamine (NBD-PE) to all lipid compositions. Lipid vesicles readily fused onto the silicon nanowires upon exposure, producing linear bright fluorescent features in the confocal microscopy images (Figure 2). The lipids used in our experiments do not form multilayers on the planar silicon oxide surfaces; for example, DOPC forms a single bilayer on both flat glass surface²⁷ and 110 nm silica nanoparticles.²⁸ In addition, line profiles of the fluorescent images of the lipid-coated nanowires (see Supporting Information, Figure S3) do not show integer multiple jumps in fluorescence intensity that would have been characteristic for lipid multilayers. Thus, we conclude that vesicle fusion produces lipid bilayers and not multilayers in our experiments. The addition of cone-shaped DOPE molecules to the lipid membrane should promote and stabilize bilayer formation on highly curved substrates and destabilize bilayers formed on the flatter substrates;²⁵ however, we observed vesicle fusion for all lipid concentrations and substrate sizes (Figure S2, Supporting Information). This observation contradicts a previous report by Hamai et al. who found that, with increasing DOPE concentration in DOPC–DOPE vesicles, the mobile fraction of supported lipid bilayers on flat surfaces dropped and fluorescence signal stopped

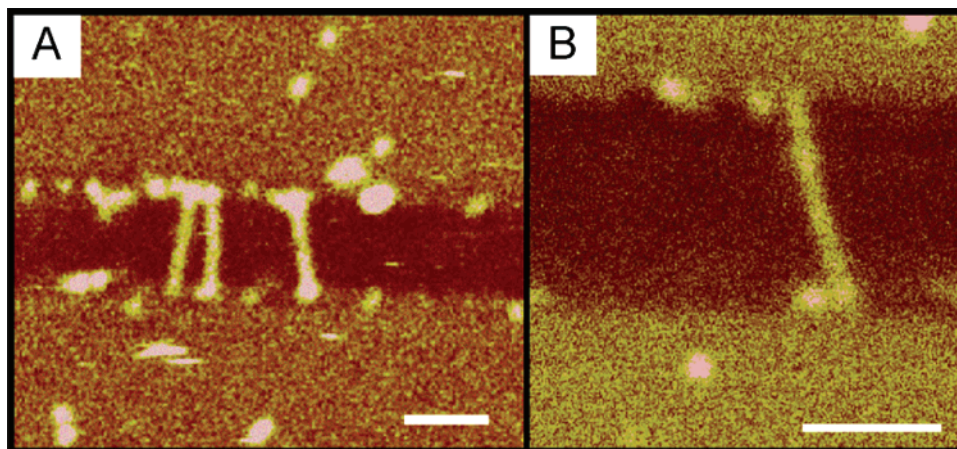


Figure 2. Confocal fluorescence microscopy images of (A) DOPC and (B) DOPC:DOPE (70:30) lipid bilayers supported on 70 nm silicon nanowires. Scale bars: 5 μm .

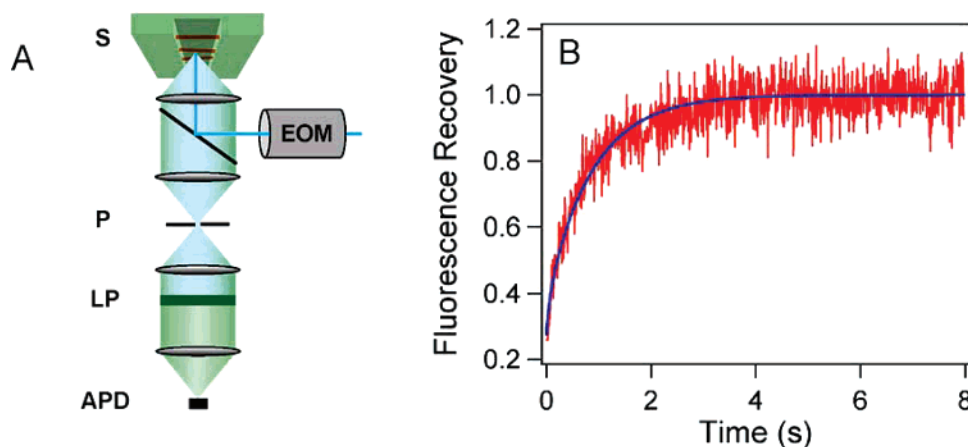


Figure 3. Mobility of the lipid bilayers supported on silicon nanowires. (A) Schematic of the experimental setup used for the FRAP measurements: S, sample; P, pinhole; LP, long pass filter; APD, avalanche photodiode detector; EOM, electro-optical modulator. (B) Representative fluorescence recovery curve (red) and the corresponding model fit (blue) for a DOPC bilayer supported on a 55 nm diameter nanowire.

recovering when the fraction of DOPE reached 20%.²⁵ The authors suggested that vesicles of this composition adsorbed on the flat substrates without fusion/bilayer formation and argued that the presence of conical DOPE molecules in the bilayer made formation of transient pores during vesicle rapture more unfavorable and thus kinetically prohibited fusion. Our results clearly demonstrate that this kinetic limitation is not insurmountable and that it is possible to form *continuous and mobile* supported bilayers (we discuss the mobility measurements in the next section) on curved surfaces of cylindrical nanowires even at DOPE fraction larger than 20%. In keeping with our experimental observations, thermodynamic analysis shows that vesicle fusion is still favorable for all substrates with diameters larger than 20 nm for all lipid compositions that we studied (see Supporting Information for details).

Lipid Mobility. Remarkably, fluorescence recovery after photobleaching (FRAP) measurements showed that our supported lipid bilayer membranes exhibited mobile fractions of nearly 100% (Figure 3b), even in membranes containing a high fraction (20–30%) of DOPE; this result also confirms

that our coatings consist of the lipid bilayers (as opposed to lipid monolayers). To measure the lipid mobility, we followed a previously described protocol,^{29,30} but to attain the time resolution necessary for capturing fast recovery processes, we incorporated a fast ($<2 \mu\text{s}$ switching time) electro-optical modulator into our setup (Figure 3a). These measurements also showed that the supported bilayers on silicon nanowires are quite robust: the fluorescence typically recovered to 90–95% of the initial value even after five bleach-recovery cycles on the same spot (data not shown). The membranes are also remarkably mobile: the diffusion coefficients of nanowire-supported membranes ($2\text{--}10 \times 10^{-8} \text{ cm}^2/\text{s}$) fall within or slightly above the range of values reported for DOPC vesicles ($5 \times 10^{-8} \text{ cm}^2/\text{s}$)³¹ and flat supported DOPC bilayers ($2\text{--}3 \times 10^{-8} \text{ cm}^2/\text{s}$).^{25,32} To eliminate the possibility of the substrate roughness contributing to the observed effects, we have performed similar mobility measurements for one-dimensional (1-D) lipid bilayers formed on the single-crystalline Si nanowires grown by VLS synthesis (see Supporting Information and Figure S5 for details). The recovery ratios and the diffusion

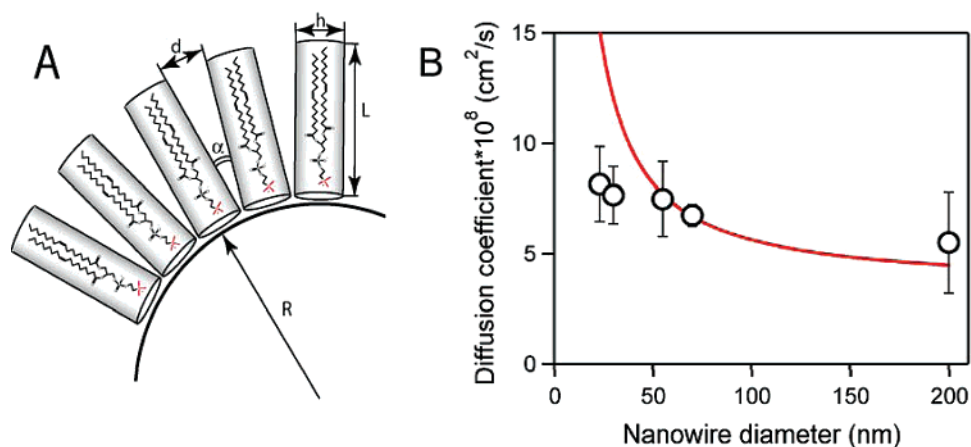


Figure 4. Comparison of the measured lipid mobility with the free space diffusion model. (A) Model schematics. Only the inner leaflet is shown for clarity. (B) Average experimental diffusion coefficients (circles) of DOPC–DOPE lipid bilayers on silicon nanowire templates and the diffusion coefficient values predicted by the eq 3 (red curve) using the following parameters: $a(T) = 0.57 \text{ nm}^2$, $M = 786 \text{ g/mol}$, $a_0 = 0.45 \text{ nm}^2$, $L = 2 \text{ nm}$, $E_a = 11.34 \text{ kJ/mol}$. All parameter values were taken from the literature.³⁶

coefficients observed in those measurements were very close to the values that we measured for the amorphous nanowire substrates.

High mobility observed in these measurements is in sharp contrast to the much lower mobility that we previously reported for one-dimensional lipid bilayers on carbon nanotube templates coated with polyelectrolytes.³⁰ These polymer substrates were of comparable size to the smallest silicon nanowires used in the present work, yet they exhibited up to 3 orders of magnitude slower diffusion coefficients. This comparison indicates that the nature of the substrate surface represents another key factor that determines the bilayer mobility on highly curved substrates.

Surprisingly, we did not observe any clear trends in mobility with changing DOPE concentration in DOPC–DOPE mixtures (see Supporting Information for mobility data for individual lipid mixtures). However, the average diffusion coefficients observed for each nanowire size show a clear trend: diffusion becomes faster for membranes supported on smaller diameter nanowires (Figure 4). The increase is fairly modest: shrinking the nanowire diameter from 200 to 20 nm increases lipid mobility by ca. 50%.

To rationalize this result, we can consider the free space model originally proposed by Cohen and Turnbull for diffusion in liquids,³³ and later adopted by Galla and colleagues for two-dimensional (2-D) diffusion in lipid bilayer membranes.³⁴ Here we use the formalism of Vaz et al., who proposed an expanded version of the 2-D model.^{35,36} This model postulates that, for the diffusion step to occur, the molecule has to have enough energy to overcome interactions with its neighbors and also have a minimum free space next to it. Combination of these two requirements leads to the following expression for the diffusion coefficient (D) of lipid molecules within the plane of the membrane:³⁶

$$D = \left(\frac{a(T)kTN_a}{8M} \right)^{1/2} \exp \left[\frac{-a_0}{a(T) - a_0} - \frac{E_a}{kT} \right] \quad (1)$$

where $a(T)$ is the average area per molecule, M is the

molecular weight, N_a is Avogadro's number, k is the Boltzmann constant, T is temperature, E_a is activation energy associated with diffusion, and a_0 is the critical area, which represents the close-packed cross-sectional molecular area. At finite temperature T , $a(T) > a_0$ and the difference $a(T) - a_0$ corresponds to the free area per molecule. If we approximate all lipid molecules packed around the nanowire circumference as rectangles (in 2-D projection), then the distance between edges of the molecules pointing away from the nanowire center (d) for small angles α is given by (Figure 4a):

$$d \approx \frac{Lh}{R} \quad (2)$$

where R is the substrate radius and L and h are the length and the width of a rectangle representing a lipid molecule, respectively. This additional separation between the molecules will add to the free space already available due to thermal motion. Because $a_0 = h^2$, the distance d corresponds to the free area $d \cdot h = La_0/R$ per molecule, which transforms eq 1 into:

$$D = \left(\frac{a(T)kTN_a}{8M} \right)^{1/2} \exp \left[\frac{-a_0}{\frac{La_0}{R} + a(T) - a_0} - \frac{E_a}{kT} \right] \quad (3)$$

This equation shows that, as the substrate diameter decreases, the lipid diffusion becomes faster. Hof et al. proposed a qualitatively similar explanation to account for faster relaxation times of a fluorescent probe in small vesicles (diameter 22 nm) compared to large ones (diameter 250 nm):³⁷ as the membrane curvature increases, the separation between lipid headgroups in the outer leaflet becomes larger and results in higher diffusion coefficients. Because all parameters in eq 3 are known, we can go one step further and directly compare the model predictions with experimental observations (Figure 4b). For the nanowire substrates with

diameters greater than 50 nm, our experimental data show good agreement with the free space model (eq 3) *with no fitting parameters*. However, the model predictions deviate from the experimental data significantly for the nanowire substrates with the diameter below 50 nm, where the model predicts faster diffusion. This comparison could indicate that the description based on the simple geometrical argument used in our model breaks down when the curvature of the membrane falls below this critical value. The measured diffusion coefficient values fall below the theoretical curve in that regime, indicating that the lipid bilayer is able to reduce the free space using different means, perhaps by redistributing the lipid molecules. As the gaps between the lipid molecules become large, the lipid tails of the second layer could also partially penetrate those gaps, thus reducing the amount of the free space and, consequently, reducing the diffusion coefficient. Additional experiments are necessary to reveal the detailed relationship between the structure and mobility of lipid bilayers in this very high curvature state.

We have shown that mixed DOPC–DOPE vesicles form supported lipid bilayers on cylindrical silicon nanowires. We demonstrate that lipid bilayers supported on these substrates are high quality, continuous, and mobile. They exhibit mobile fractions of 90–100% and diffusion coefficients close to typical values observed for DOPC membranes supported on flat silicon oxide surfaces. We also found that the membrane mobility increases systematically as the nanowires become thinner. The free space diffusion model provides a good description of the effect of substrate curvature on lipid mobility for nanowires above 50 nm in diameter but grossly overestimates the effect for thinner nanowires.

One-dimensional bilayers on high-curvature solid supports provide a reliable platform for studying fundamental physical properties of the highly curved lipid bilayers. Use of these model systems opens up a number of opportunities for researchers to study the fundamental role of lipid bilayer curvature in biological processes related to disease, signaling, and cell cycle. One of the advantages of our approach is that it provides a highly controllable and robust tubular lipid bilayer platform in the curvature regime that was previously difficult to access in the laboratory setting. Our lipid bilayer systems are stable and easy to manipulate and characterize using a variety of techniques. The experimental approach that we present is quite general and should also work for other types of hydrophilic nanowires, demonstrating that 1-D lipid bilayers provide a versatile platform for integration of biological membranes with 1-D nanomaterials.

Acknowledgment. S.C.J.H., A.B.A., and J.A.M. acknowledge support from the SEGRF program at LLNL. D.J.S. acknowledges funding from H. Graboske Postdoctoral Fellowship Program at LLNL. A.N. acknowledges funding from LLNL LSTO. This work was performed under the auspices of the U.S. Department of Energy by the University of California, Lawrence Livermore National Laboratory, under contract no. W-7405-Eng-48.

Supporting Information Available: Materials and methods, thermodynamics of bilayer formation, mobility of one-dimensional lipid bilayers on crystalline VLS silicon nanowires

References

- (1) Cluett, E. B.; Wood, S. A.; Banta, M.; Brown, W. J. *J. Cell Biol.* **1993**, *120*, 15–24.
- (2) McNiven, M. A.; Thompson, H. M. *Science* **2006**, *313*, 1591–1594.
- (3) Sciak, N.; Presley, J.; Smith, C.; Zaal, K. J. M.; Cole, N.; Moreira, J. E.; Terasaki, M.; Siggia, E.; Lippincott-Schwartz, J. *J. Cell Biol.* **1997**, *139*, 1137–1155.
- (4) Conner, S. D.; Schmid, S. L. *Nature* **2003**, *422*, 37–44.
- (5) Farsad, K.; Ringstad, N.; Takei, K.; Floyd, S. R.; Rose, K.; De Camilli, P. *J. Cell Biol.* **2001**, *155*, 193–200.
- (6) Peter, B. J.; Kent, H. M.; Mills, I. G.; Vallis, Y.; Butler, P. J. G.; Evans, P. R.; McMahon, H. T. *Science* **2004**, *303*, 495–4499.
- (7) McMahon, H. T.; Gallop, J. L. *Nature* **2005**, *438*, 590–596.
- (8) Zimmerberg, J.; Kozlov, M. M. *Nat. Rev. Mol. Cell Biol.* **2006**, *7*, 9–19.
- (9) Parthasarathy, R.; Groves, J. T. *Soft Matter* **2007**, *3*, 24–33.
- (10) Kucerka, N.; Pencser, J.; Sachs, J. N.; Nagle, J. F.; Katsaras, J. *Langmuir* **2007**, *23*, 1292–1299.
- (11) Sykora, J.; Jurkiewicz, P.; Epand, R. M.; Kraayenhof, R.; Langner, M.; Hof, M. *Chem. Phys. Lipids* **2005**, *135*, 213–221.
- (12) Parthasarathy, R.; Yu, C.; Groves, J. T. *Langmuir* **2006**, *22*, 5095–5099.
- (13) Roux, A.; Cuvelier, D.; Nassoy, P.; Prost, J.; Bassereau, P.; Goud, B. *EMBO J.* **2005**, *24*, 1537–1545.
- (14) Schindler, M.; Koppel, D. E.; Sheetz, M. P. *Proc. Natl. Acad. Sci. U.S.A.* **1980**, *77*, 1457–1461.
- (15) Schlessinger, J.; Shechter, Y.; Cuatrecasas, P.; Willingham, M. C.; Pastan, I. *Proc. Natl. Acad. Sci. U.S.A.* **1978**, *75*, 5353–5357.
- (16) Kochy, T.; Bayerl, T. M. *Phys. Rev. E* **1993**, *47*, 2109–2116.
- (17) Picard, F.; Paquet, M. J.; Dufourc, E. J.; Auger, M. *Biophys. J.* **1998**, *74*, 857–868.
- (18) de Figueiredo, P.; Drecktrah, D.; Katzenellenbogen, J. A.; Strang, M.; Brown, W. J. *Proc. Natl. Acad. Sci. U.S.A.* **1998**, *95*, 8642–8647.
- (19) Roux, A.; Cappello, G.; Cartaud, J.; Prost, J.; Goud, B.; Bassereau, P. *Proc. Natl. Acad. Sci. U.S.A.* **2002**, *99*, 5394–5399.
- (20) Takei, K.; Haucke, V.; Slepnev, V.; Farsad, K.; Salazar, M.; Chen, H.; De Camilli, P. *Cell* **1998**, *94*, 131–141.
- (21) Sackmann, E. *Science* **1996**, *271*, 43–48.
- (22) Cremer, P. S.; Boxer, S. G. *J. Phys. Chem. B* **1999**, *103*, 2554–2559.
- (23) Morales, A. M.; Lieber, C. M. *Science* **1998**, *279*, 208–211.
- (24) Cui, Y.; Lauhon, L. J.; Gudiksen, M. S.; Wang, J.; Lieber, C. M. *Appl. Phys. Lett.* **2001**, *78*, 2214–2216.
- (25) Hamai, C.; Yang, T.; Kataoka, S.; Cremer, P. S.; Musser, S. M. *Biophys. J.* **2006**, *90*, 1241–1248.
- (26) Cooke, I. R.; Deserno, M. *Biophys. J.* **2006**, *91*, 487–495.
- (27) Richter, R.; Mukhopadhyay, A.; Brisson, A. *Biophys. J.* **2003**, *85*, 3035–3047.
- (28) Mornet, S.; Lambert, O.; Duguet, E.; Brisson, A. *Nano Lett.* **2005**, *5*, 281–285.
- (29) Axelrod, D.; Koppel, D. E.; Schlessinger, J.; Elson, E.; Webb, W. W. *Biophys. J.* **1976**, *16*, 1055–1069.
- (30) Artyukhin, A. B.; Shestakov, A.; Harper, J.; Bakajin, O.; Stroeve, P.; Noy, A. *J. Am. Chem. Soc.* **2005**, *127*, 7538–7542.
- (31) Toccanne, J. F.; Dupouzezanne, L.; Lopez, A. *Prog. Lipid Res.* **1994**, *33*, 203–237.
- (32) Przybylo, M.; Sykora, J.; Humpolickova, J.; Benda, A.; Zan, A.; Hof, M. *Langmuir* **2006**, *22*, 9096–9099.
- (33) Cohen, M. H.; Turnbull, D. *J. Chem. Phys.* **1959**, *31*, 1164–1169.
- (34) Galla, H. J.; Hartmann, W.; Theilen, U.; Sackmann, E. *J. Membr. Biol.* **1979**, *48*, 215–236.
- (35) Vaz, W. L. C.; Clegg, R. M.; Hallmann, D. *Biochemistry* **1985**, *24*, 781–786.
- (36) Almeida, P. F. F.; Vaz, W. L. C.; Thompson, T. E. *Biochemistry* **1992**, *31*, 6739–6747.
- (37) Hof, M.; Hutterer, R.; Perez, N.; Ruf, H.; Schneider, F. W. *Biophys. Chem.* **1994**, *52*, 165–172.

NL071641W